A. GRAJCAR*, P. SKRZYPCZYK*, D. WOŹNIAK**

THERMOMECHANICALLY ROLLED MEDIUM-Mn STEELS CONTAINING RETAINED AUSTENITE

WALCOWANE TERMOMECHANICZNIE STALE ŚREDNIOMANGANOWE ZAWIERAJĄCE AUSTENIT SZCZĄTKOWY

Chemical composition of four medium-Mn steels containing a various Mn content (3 and 5%) have been proposed in the present work. The two steels are base steels whereas the other two contain Nb microaddition. Thermomechanical rolling tests of 3.3 mm sheets have been carried out using a semi-industrial hot strip rolling line. Detailed investigations of the identification of structural constituents using light microscopy and scanning electron microscopy techniques have been performed. X-ray method has been applied to determine an amount of retained austenite and its C content. Significant microstructural parameters were revealed using an EBSD technique. It was found that the Mn addition affects strongly a microstructure type, stability of retained austenite and mechanical properties determined with a static tensile test. The steels containing 3% Mn are characterized by a good combination of strength and ductility whereas the tensile strength up to 1300 MPa is possible to obtain for the higher Mn content steels.

Keywords: medium-Mn steel, bainitic steel, thermomechanical rolling, retained austenite stability, controlled cooling

W pracy zaprojektowano cztery składy chemiczne stali średniomanganowych zawierających 3 i 5% Mn. Dwie stale to stale bazowe, a pozostałe dwie zawierają mikrododatek Nb. Przeprowadzono próby walcowania termomechanicznego taśm o grubości 3.3 mm, stosując półprzemysłową linię walcowania na gorąco. Przeprowadzono szczegółowe badania identyfikacji składników strukturalnych z zastosowaniem mikroskopii świetlnej i skaningowej mikroskopii elektronowej. Udział austenitu szczątkowego i stężenie C w tej fazie wyznaczono metodą rentgenowską. Metoda EBSD została użyta do ilościowego wyznaczenia istotnych parametrów mikrostrukturalnych. Stwierdzono, że dodatek Mn ma silny wpływ na rodzaj otrzymanej mikrostruktury, stabilizację austenitu szczątkowego oraz własności mechaniczne wyznaczone w statycznej próbie rozciągania. Stale zawierające 3% Mn charakteryzują się dobrym połączeniem wytrzymałości i plastyczności, a stale o wyższym stężeniu Mn pozwalają uzyskać wytrzymałość na rozciąganie do 1300 MPa.

1. Introduction

Automotive industry needs lightweight materials showing a good combination of strength and ductility. Recently, the pressure is especially directed to improve crashworthiness of a car's structure using sheets with strength levels between 700 and 1200 MPa without loss of formability. These rigorous requirements are met by a new class of advanced steels developed during last two decades. The 1st generation AHSS (Advanced High Strength Steels) include different multiphase steels utilizing a composite-like behaviour to obtain a desired balance between strength and formability [1-4]. These sheet steels containing ferrite, bainite, martensite and retained austenite at various combinations and proportions are successfully produced in the industry for a few years. The 2nd generation AHSS are characterized by a superior balance between strength and plasticity due to TRIP (TRansformastion Induced Plasticity) or TWIP (Twinning Induced Plasticity) effects [5-7]. These high-manganese steels show a single-phase austenitic microstructure and contain a high content of alloying elements (20-30% Mn, 1-3% Si, 1-3% Al). At present, industrial trials are carried out to employ them for some crash-relevant elements of a body-in-white. Recently, the 3rd generation AHSS have been evolved in answer to the demand of the automotive industry for cost-efficient steels [8-13].

The 3rd generation AHSS cover different medium-Mn steels showing TRIP and TWIP effects as major work hardening mechanisms. The manganese content is reduced to a range between 3 and 12%. Steels containing from about 3 to 5% are usually processed using Quenching and Partitioning (QP) treatment [12 13]. The main idea of the process is to stabilize retained austenite through its enrichment in carbon from martensite produced between M_s and M_f temperatures. A higher fraction of retained austenite (between 15 and 45%) can be produced using intercritical annealing after cold rolling of low-carbon martensitic microstructure sheet steels. These steels contain between 5 and 12% Mn and their strength-ductility balance (due to TRIP and TWIP effects) is similar to that of high-manganese steels [8, 9, 11, 13, 14]. The idea is to obtain an ultra fine-grained ferrite-austenite

 *   SILESIAN UNIVERSITY OF TECHNOLOGY, INSTITUTE OF ENGINEERING MATERIALS AND BIOMATERIALS, 18A KONARSKIEGO STR., 44-100 GLIWICE, POLAND

**   INSTITUTE FOR FERROUS METALLURGY, 12-14 K. MIARKI STR., 44-100 GLIWICE, POLAND

microstructure and to stabilize a γ phase through C and Mn partitioning from ferrite into austenite and grain refinement. Unfortunately, the main disadvantage of the process is a long annealing time required for diffusive enrichment of austenite in manganeze. Therefore, efficient continuous annealing lines should be replaced by batch annealing. Additionally, the Luders elongation and PLC effect are real problems during stamping of industrial sheets.

An alternative for cold-rolled sheets are products produced by thermomechanical rolling using modern hot strip rolling lines equipped with laminar cooling facilities. Thermomechanical processing of ultra-high strength medium-Mn steel sheets have not been investigated to a wide extent so far [15, 16]. Recently, Grajcar et al. simulated hot strip rolling of medium-Mn steels using a Gleeble simulator [16] and a semi-industrial thermomechanical rolling line. Their reported that it is possible to obtain good-quality sheet products but the processing requires taking into account increased flow stresses and rolling forces [17]. The aim of the present work is to characterize in detail the microstructure of thermomechanically rolled 3% Mn and 5% Mn steels.

2. Experimental

The chemical composition of vacuum-melted medium-Mn steels is given in Table 1. The concentration of Mn, Al and Nb is the basis for steel coding (3Mn-1.5Al, 3Mn-1.5Al-Nb, 5Mn-1.5Al and 5Mn-1.5Al-Nb). Manganese was used to stabilize retained austenite whereas the high-Al concept was chosen to prevent carbide precipitation. Mo and Nb were used to increase a strength level. The ingots were hot-forged and roughly rolled to a thickness of 8.5 mm.

TABLE 1

Chemical composition of the investigated steels (wt. %)

Steel code	C	Mn	Al	Si	Mo	Nb	S	P
3Mn-1.5Al	0.17	3.3	1.7	0.22	0.23	–	0.014	0.010
3Mn-1.5Al-Nb	0.17	3.1	1.6	0.22	0.22	0.04	0.005	0.008
5Mn-1.5Al	0.16	4.7	1.6	0.20	0.20	–	0.004	0.008
5Mn-1.5Al-Nb	0.17	5.0	1.5	0.21	0.20	0.03	0.005	0.008

Thermomechanical rolling was carried out at the Institute for Ferrous Metallurgy (Gliwice, Poland) using the semi-industrial hot-rolling line consisted of the two-high reversing mill, isothermal heating panels located before and after a rolling stand, a cooling device and a run-out table [17, 18]. Hot-rolling included 5 deformation steps to a final sheet thickness of 3.3 mm. An austenitizing temperature was 1200°C and a finishing rolling temperature was equal to about 750°C. Slightly different cooling strategies were used for 3Mn and 5Mn steels due to their different hardenability. The steel sheets containing 3% Mn were initially slowly cooled within 5 s to about 700°C to investigate if ferrite is formed or not (Fig. 1a). The next step included the controlled mixed air-blow and water-spray cooling to 400°C. The samples were isothermally held in the furnace for 300 s to enrich austenite in carbon. The

last step consisted of air cooling of sheets to room temperature. The cooling schedule for the steels containing 5% Mn was simple. The sheet samples were directly cooled to 400°C following finishing rolling to obtain bainite-based microstructures (Fig. 1b).

Standard size A50 tensile test samples with a gauge length of 50 mm and a width of 12.5 mm were cut parallel to the rolling direction of sheets. The static tensile test was carried out at a strain rate of 5×10^{-3} s^{-1}. Metallographic specimens were taken along the rolling direction. For a detailed microstructural analysis, the methods of light microscopy (LM), scanning electron microscopy (SEM) and the orientation imaging microscopy (OIM) using SEM were applied. Etching in 10% aqueous solution of sodium metabisulfite was used. Metallographic observations at magnification of 1000x were carried out with a Leica MEF 4A light microscope. Morphological details of the microstructure were revealed with the SUPRA 25 SEM using back-scattered electrons (BSE). Observations were carried out on nital-etched samples at the accelerating voltage of 20kV. The EBSD technique was performed by the use of the Inspect F SEM equipped with the Shottky's field emission. After classical grinding and polishing, specimens were polished with Al_2O_3. The final step of sample preparation was their ion polishing using the GATAN 682 PECS system.
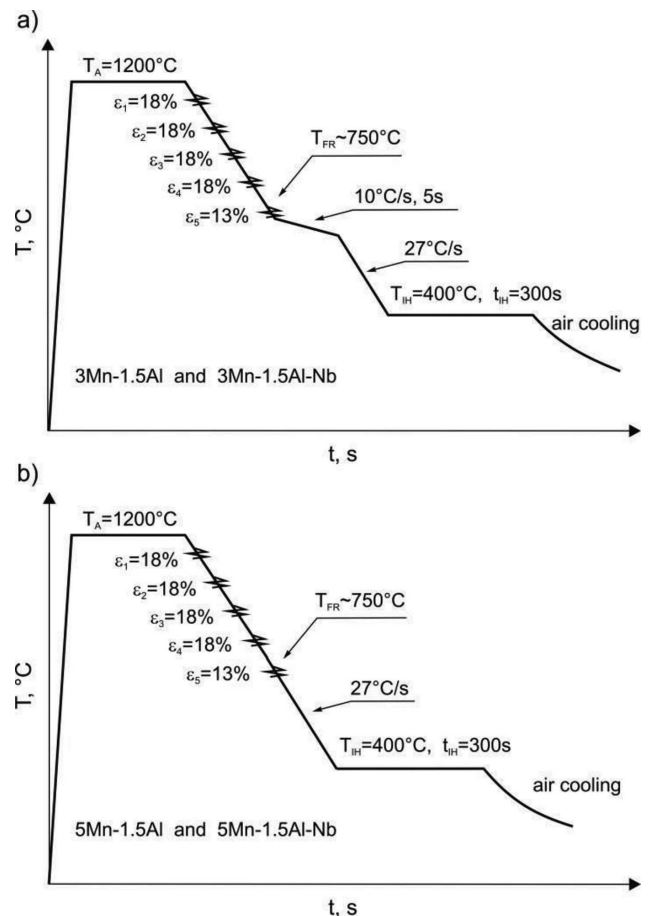

Fig. 1. Thermomechanical rolling schedules of 8.5 mm thick sheet samples to a thickness of 3.3 mm for the steels containing 3% Mn (a) and 5% Mn (b); T_A – austenitizing temperature, T_{FR} – finishing rolling temperature, T_{IH} – isothermal holding temperature, t_{IH} – isothermal holding time

Retained austenite amount was determined using the X-ray quantitative analysis and EBSD technique. Carbon concentration in the retained austenite (C_γ) was estimated on the basis of positions of the diffraction line maxima using the following formula: $a_\gamma = 0.3578 + 0.0033C_\gamma$, where a_γ is the lattice parameter of retained austenite (nm). X-ray investigations were carried out with the filtered Co radiation and an X-pert PRO diffractometer operating at 40 kV and 30 mA, equipped with an X'Celerator detector. Three alpha and four gamma peaks were quantified by scanning trough a 2-theta range from 40 to 115 deg.

3. Results and discussion

3.1. Microstructure characterization

A microstructure of the 3Mn steel consists of bainite and retained austenite (Fig. 2a). Polygonal ferrite can be hardly found due to a strong hardenability effect of Mn addition. A microstructure of the 5Mn steel shows a more lath-like morphology (Fig. 2b). It contains bainite, martensite and retained austenite. There is no polygonal ferrite in the microstructure. Both microstructures are characterized by the high grain refinement. It can be seen that in a prior austenite grain a few bainite-martensite colonies of high dispersion are formed.
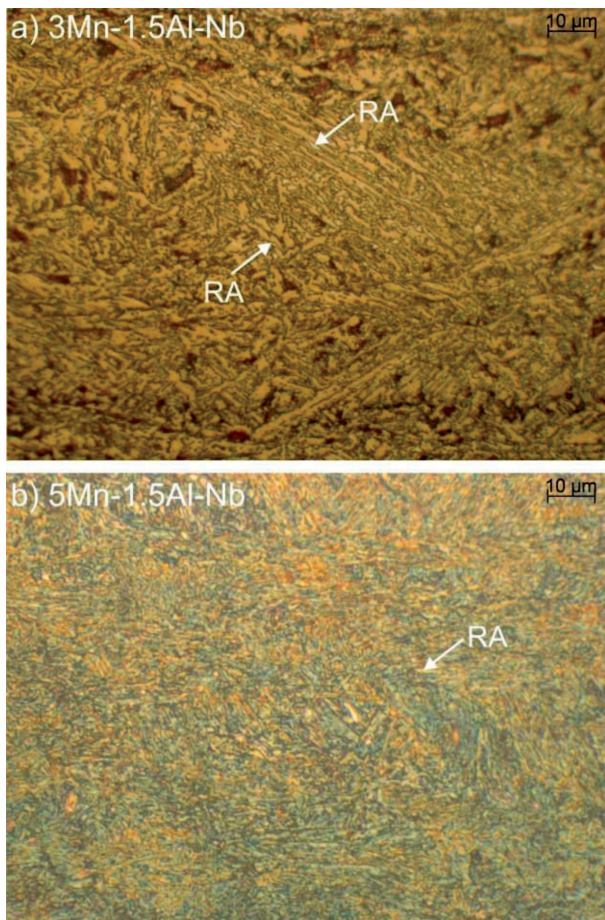

Fig. 2. Microstructure of the thermomechanically processed 3Mn-1.5Al-Nb (a) and 5Mn-1.5Al-Nb steels (b); RA – retained austenite
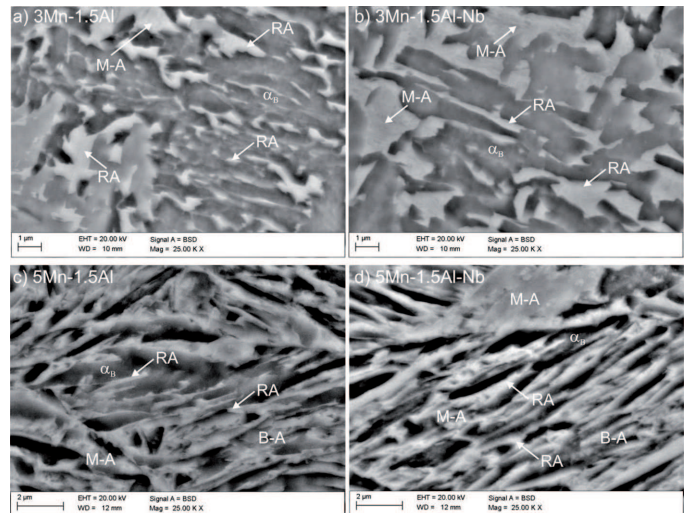

Fig. 3. SEM micrographs showing the morphology of structural constituents in 3Mn-1.5Al (a), 3Mn-1.5Al-Nb (b), 5Mn-1.5Al (c) and 5Mn-1.5Al-Nb steels (d); RA – retained austenite, α_B – bainitic ferrite, M-A – martensite-austenite constituents, B-A – bainite-austenite constituents

A more detailed analysis can be carried out using SEM. Figures 3a and 3b show the microstructures of the steels containing 3% Mn. Usually, niobium microaddition causes grain refinement [19, 20]. In the present case, it seems that Nb addition does not have a distinct effect on the microstructure of the investigated steels. Our earlier results indicated that niobium is dissolved in solid solution because of hampering effects of Mn and Al on carbide precipitation [10, 16]. Small granules and interlath retained austenite can be seen between laths of bainitic ferrite. It is clearly visible that totally stable is only interlath retained austenite. Larger blocky austenite grains with a size above 2 μm transformed during cooling of steel to room temperature forming martensite-austenite (M-A) constituents. The martensitic transformation takes place in central parts of the islands as a result of their smaller enrichment in carbon than external regions. Interlath retained austenite is a major morphological type of the γ phase in the steels containing 5% Mn. It is a typical morphology of γ phase in isothermally treated bainitic alloys [21]. Retained austenite is located between bainitic ferrite laths forming bainitic-austenitic (B-A) constituents (Fig. 3c and d).

Further microstructural details and quantitative data can be revealed by analysing EBSD maps in Fig. 4. The brightest grains in the image quality (IQ) map represent bainite areas (Fig. 4a). Retained austenite, martensite and grain boundaries are represented by different levels of the dark grey because their pattern contrast is lower than that of bainitic ferrite. The phase map (Fig. 4b) confirms that austenite regions are fragmented forming M-A constituents. The low finishing rolling temperature of 750°C results in a large amount of low-angle boundaries in Fig. 4c. In fact, their number fraction is slightly larger when compared to the high-angle boundaries. It is the confirmation of advancing the dislocation substructure during thermomechanical rolling [22]. A relatively large fraction of retained austenite exhibits misorientation angles close to 45° with neighbouring BCC constituents (Fig. 5). It indicates the presence of the Kurdjumov-Sachs (K-S) and Nishiyama-Wasserman (N-W) relationships between bainitic
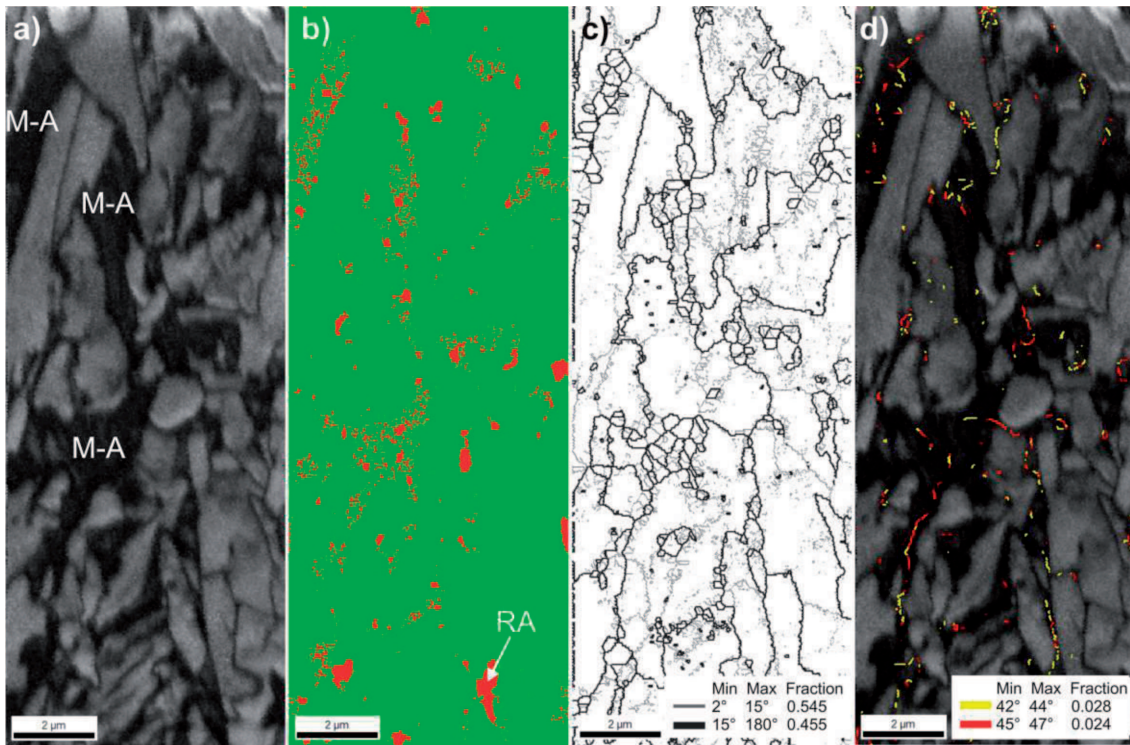
Fig. 4. Image quality (IQ) map (a), colour-coded phase map (b), misorientation angles showing high-angle boundaries (thick lines) and low-angle boundaries (thin lines) (c) and IQ map with misorientation angles corresponding to the Kurdjumov-Sachs (42-44°, in yellow) and Nishiyama-Wasserman (45-47°, in red) relationships (d); 3Mn-1.5Al steel, M-A – martensite-austenite constituents, RA – retained austenite
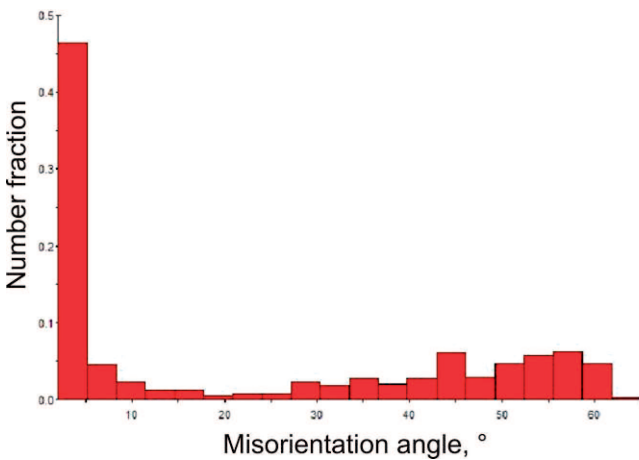

Fig. 5. Distribution of misorientation angles of 3Mn-1.5Al steel

Fig. 6. Distribution of image quality values of 3Mn-1.5Al steel

ferrite and retained austenite. These relationships can be expressed by specific parallel directions and planes as well as characteristic misorientation angles between α and γ phases. The angles are sufficiently different to be distinguished using the EBSD mapping [23]. Hence, they are marked in Fig. 4d.

Two distinct peaks can be identified in Fig. 6 showing the distribution of image quality values from Fig. 4. It is clear that the first peak in a range of 150-250 corresponds to martensite and martensite-austenite constituents. Martensite is the most defective phase. Thus, its diffraction quality is very poor [24]. Bainitic ferrite contains a lower density of structural defects, what results in higher IQ values. A lower stability of retained austenite in the steels containing 5% Mn is confirmed by EBSD maps in Fig. 7. Retained austenite is strongly fragmented forming numerous M-A constituents embedded between bainitic ferrite laths.
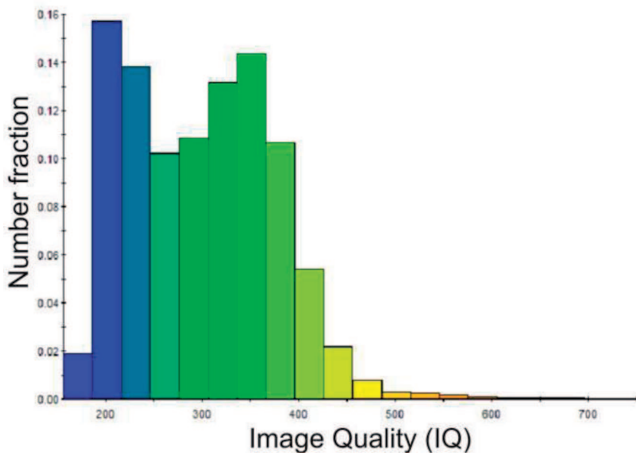
3.2. Retained austenite amount

The amount of retained austenite determined by XRD and EBSD techniques is listed in Table 2. It is interesting that the volume fraction of retained austenite is higher for the steels containing a lower Mn content. The explanation of this is the carbon concentration in the γ phase. The C content is higher for the 3Mn-1.5Al and 3Mn-1.5Al-Nb steels. It is in accordance with the equilibrium considerations carried out by Gioti et al. [25] for medium-Mn steels containing 0.2% C and 2% Al. Their thermodynamic calculations revealed that the steel containing 5% Mn is more enriched in carbon compared to the steel containing 8% Mn. These calculations are confirmed by experimental results of Sugimoto et al. [26] in TRIP-aided steels containing from 1 to 2.5% Mn. Recently, Sugimoto et

al. [27] confirmed this dependence in medium-Mn steels for a manganese range from 1.5 to 5%. The lower C content in the present steels containing 5% Mn reveals as the occurrence of numerous M-A constituents, which indicate the lower stability of γ phase (Fig. 3c, d, Fig. 7) when compared to the steels containing 3% Mn.
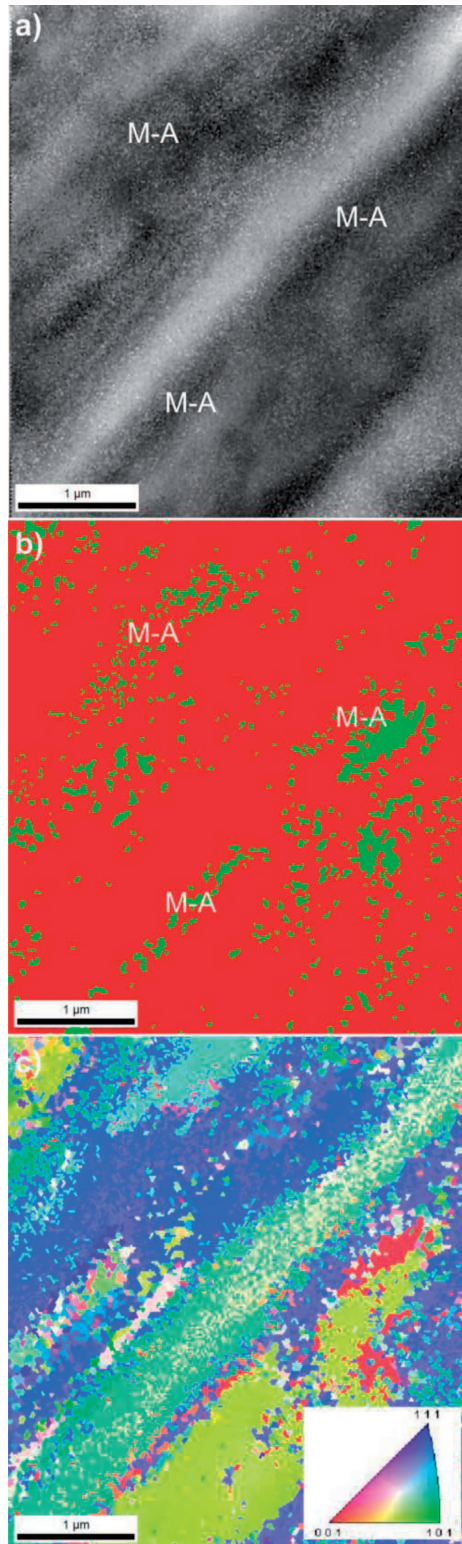

Fig. 7. Image quality (IQ) map (a), colour-coded phase map (b) and orientation map (c) showing martensite-austenite (M-A) constituents in the 5Mn-1.5Al steel

Retained austenite amount estimated by the EBSD method is slightly smaller than the volume fractions determined by the XRD (Table 2). It is typical due to the lack of indexing the smallest particles of retained austenite and austenite films in contrary to X-ray investigations [23, 24]. It should be noted the C content in retained austenite is a little bit smaller for Nb-bearing steels. This dependence was also observed by Krizan and De Cooman [1, 3]. It is due to carbides' precipitation. It was reported earlier [10, 16] that both Mn and Al additions prevent the precipitation of Nb carbonitrides. However, this process can be initiated especially in the steel containing 3% Mn.

TABLE 2

Retained austenite amount and other parameters describing retained austenite

Steel code	Retained austenite amount, %		Lattice constant, a_γ, nm	C content in austenite, C_γ, wt. %	$f_{\gamma 0} \times C_\gamma$, wt. %
	EBSD	XRD			
3Mn-1.5Al	16.5	17.7	0.36182	1.22	0.216
3Mn-1.5Al-Nb	14.0	15.5	0.36143	1.10	0.170
5Mn-1.5Al	8.1	9.6	0.36124	1.04	0.100
5Mn-1.5Al-Nb	7.4	8.3	0.36110	1.00	0.083

3.3. Mechanical properties

Mechanical properties of the steels are listed in Table 3. The steels containing lower contents of Mn are characterized by higher ductility whereas the 5Mn-1.5Al and 5Mn-1.5Al-Nb steels have very high strength levels. The yield stress of 3Mn steels is near 700 MPa and above 200 MPa higher for the steels containing 5% Mn. This property is higher for Nb-containing steels. On the other hand, the ultimate tensile strength and elongation are less dependent on Nb microaddition but they are dependent on a progress of strain-induced martensitic transformation. The $YS_{0.2}$/UTS ratio is equal to about 0.7 for all the steels. It indicates their strong strain hardening potential. It is clear from Table 2 that the 3Mn-1.5Al and 3Mn-1.5Al-Nb steels have higher $f_{\gamma 0} \times C_\gamma$ product values. Therefore, their total elongation is near 15%. The lower volume fraction and C content in retained austenite as well as the occurrence of numerous M-A constituents in the 5Mn steels lead to high UTS values of about 1300 MPa but the ductility is lower when compared to the steels containing 3% Mn (Table 3).

TABLE 3

Mechanical properties of the investigated steels

Steel code	$YS_{0.2}$, MPa	UTS, MPa	A_{50}, %	A_g, %	$YS_{0.2}$/ UTS	$UTS \cdot A_{50}$, MPa·%
3Mn-1.5Al	684	986	14.8	13.2	0.69	14593
3Mn-1.5Al-Nb	698	997	14.0	12.1	0.70	13958
5Mn-1.5Al	901	1259	8.0	6.2	0.71	10072
5Mn-1.5Al-Nb	942	1310	9.2	6.9	0.72	12052

Mechanical properties are directly related to the mechanical stability of retained austenite upon straining [28-30]. It is clear that mechanical stability of retained austenite is lower in the steels containing 5% Mn. It is confirmed by a shape of stress-strain curves in Fig. 8a showing the enhanced work strengthening for 5Mn steels and more gradual increase of stress for the steels containing lower Mn contents.
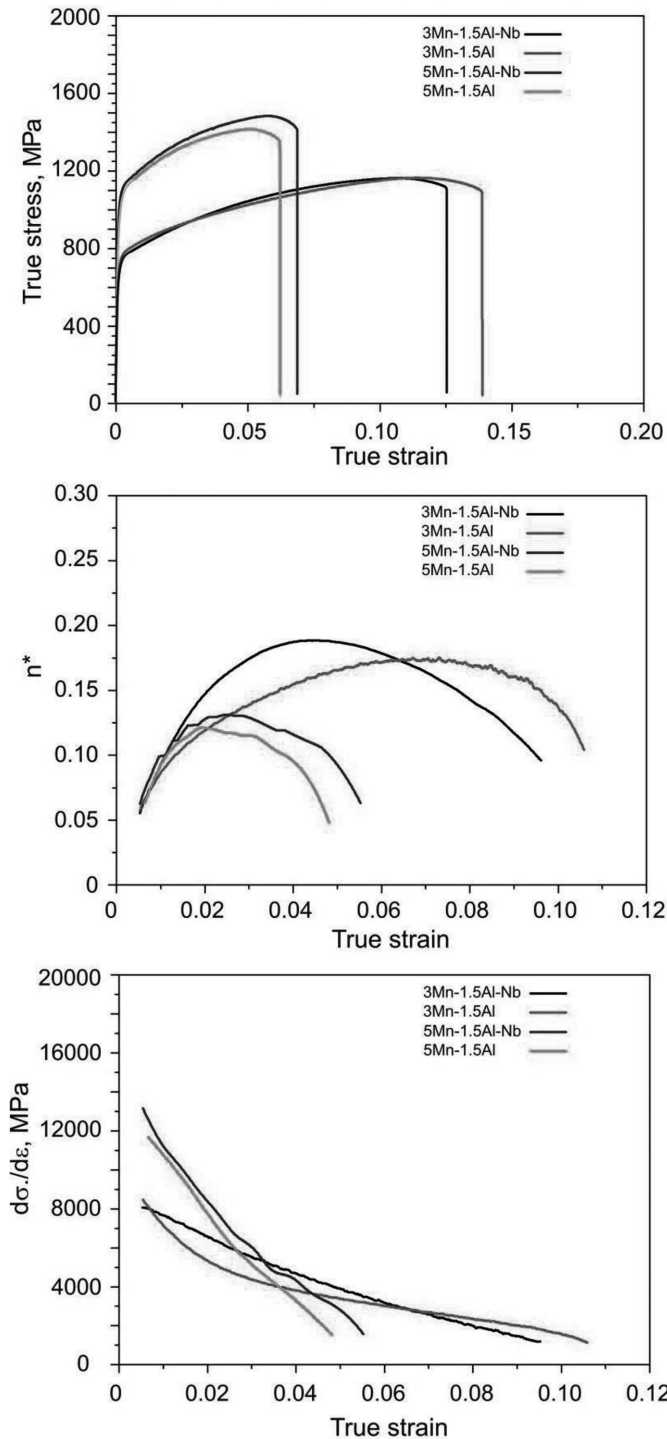

Fig. 8. True stress-true strain curves (a), instantaneous work hardening exponent values (b) and work hardening rate as a function of true strain (c)

Completing rolling at a low temperature of 750°C leads to a strong strain hardening of sheets. It is the reason of relatively low values of instanteneous work hardening exponent in

a range between 0.12 and 0.18. The consequence of a higher strength level of 5Mn steels is their lower ability to be further hardened. The n* values raise gradually and are higher for the 3Mn-1.5Al and 3Mn-1.5Al-Nb steels (Fig. 8b). The work hardening exponent increases to a strain of about 0.07. Near stable value of this exponent confirms that the material is hardened as a result of the TRIP effect. The gradual progress of strain-induced martensitic transformation reveals as a delayed necking. After that, a further decrease of the work hardening exponent indicates that the material can not accommodate additional strain, what leads to fracture. The work hardening rate of all steels is high at low strains (Fig. 8c). Its value is higher for the steels containing 5% Mn. Unfortunately, $d\sigma/d\varepsilon$ decreases rapidly for these steels. On the other hand, the decrease is more gradual for the 3Mn-1.5Al and 3Mn-1.5Al-Nb steels, what results in better ductility values.

4. Conclusions

The thermomechanical rolling schedules have been proposed for a new group of medium-Mn automotive sheet steels containing 3 and 5% Mn. Al addition prevented carbide precipitation during isothermal holding of steel at 400°C. Hence, different morphological mixtures of bainitic ferrite and retained austenite were produced dependent on the Mn content. It was proved that the increase of Mn content from 3 to 5% destabilizes the γ phase due to its smaller enrichment in carbon. The similar effect has Nb microaddition but to a lesser extent than a manganese addition. The 3Mn steels have a microstructure of bainitic ferrite with interlath and blocky retained austenite whereas martensite-austenite constituents are located between bainitic ferrite laths in the steels containing 5% Mn. The presence of about 17% retained austenite sufficiently enriched in carbon ($C_\gamma \sim 1.2$ wt.%) in the steels containing 3% Mn allows obtaining high yield strength levels of about 700 MPa and UTS up to 1000 MPa at satisfactory elongation ($A_{50} \sim 15\%$). The increase of Mn content to 5% leads to ultra high strength levels ($YS_{0.2} > 900$ MPa, UTS ~ 1300 MPa) but the low mechanical stability of retained austenite results in smaller ductility of steel sheets ($A_{50} \sim 9\%$).

REFERENCES

[1] D. K r i z a n, B.C. D e C o o m a n, Steel Res. Int. **79**, 7, 513 (2008).
[2] K. S u g i m o t o, T. I i d a, J. S a k a g u c h i, T. K a s h i m a, ISIJ Int. **40**, 9, 902 (2000).
[3] D. K r i z a n, B.C. D e C o o m a n, Metall. Mater. Trans. A **45A**, 3481 (2014).
[4] M. A d a m c z y k, D. K u c, E. H a d a s i k, Arch. Civ. Mech. Eng. **8**, 3, 5 (2008).
[5] A. G r a j c a r, M. O p i e l a, G. F o j t - D y m a r a, Arch. Civ. Mech. Eng. **9**, 3, 49 (2009).
[6] M. J a b ł o ń s k a, G. N i e w i e l s k i, R. K a w a l l a, Solid State Phenom. **212**, 87 (2014).
[7] L.A. D o b r z a ń s k i, W. B o r e k, Arch. Civ. Mech. Eng. **12**, 3, 299 (2012).
[8] S.J. L e e, S. L e e, B.C. D e C o o m a n, Scripta Mater. **64**, 649 (2011).

[9] P.J. Gibbs, E. De Moor, M.J. Merwin, B. Clausen, J.G. Speer, D.K. Matlock, Metall. Mater. Trans. A **42**, 3691 (2011).

[10] A. Grajcar, R. Kuziak, Adv. Mater. Res. **314-316**, 119 (2011).

[11] J. Shi, X. Sun, M. Wang, W. Hui, H. Dong, W. Cao, Scripta Mater. **63**, 815 (2010).

[12] H. Jirkova, B. Masek, M.F.X. Wagner, D. Langmajerova, L. Kucerova, R. Treml, D. Kiener, J. Alloys Comp. (2013), doi.org/10.1016/j.jallcom.2013.12.028.

[13] S. Lee, B.C. De Cooman, Metall. Mater. Trans. A **45A**, 709 (2014).

[14] C. Wang, J. Shi, C.Y. Wang, W.J. Hui, M.Q. Wang, ISIJ Int. **51**, 4, 651 (2011).

[15] E.I. Poliak, D. Bhattacharya, Mater. Sci. Forum **783-786**, 3 (2014).

[16] A. Grajcar, P. Skrzypczyk, R. Kuziak, K. Gołombek, Steel Res. Int. **85**, 6, 1058 (2014).

[17] A. Grajcar, P. Skrzypczyk, D. Woźniak, S. Kołodziej, J. Achiev. Mater. Manuf. Eng. **57**, 1, 38 (2013).

[18] B. Garbarz, W. Burian, D. Woźniak, Steel Res. Int., Special Edition: Metal Forming 2012, 1251 (2012).

[19] M. Opiela, Mater. Tehnol. **48**, 4, 587 (2014).

[20] M. Opiela, A. Grajcar, Arch. Civ. Mech. Eng. **12**, 4, 427 (2012).

[21] P. Pawluk, E. Skołek, M. Kopcewicz, W. Świątnicki, Solid State Phenom. **203-204**, 150 (2013).

[22] A. Basuki, E. Aernoudt, J. Mater. Proc. Tech. **89-90**, 37 (1999).

[23] S. Zaefferer, J. Ohlert, W. Bleck, Acta Mater. **52**, 2765 (2004).

[24] A.J. De Ardo, C.I. Garcia, K. Chuo, M. Hua, Mater. Manuf. Proc. **25**, 33 (2010).

[25] E. Gioti, H. Kamoutsi, G.N. Haidemenopoulos, A computational study of Mn and C stabilization of retained austenite in medium-Mn TRIP steels, in: W. Bleck, D. Raabe (Eds.), Proc. of 2nd Int. Conf. on High Manganese Steel 2014, Aachen, 337 (2014).

[26] K. Sugimoto, N. Usui, M. Kobayashi, S. Hashimoto, ISIJ Int. **32**, 1311 (1992).

[27] K. Sugimoto, H. Tanino, J. Kobayashi, Impact toughness of 0.2%C-1.5Si-1.5Mn-5.0Mn TRIP-aided martensitic steels, in: W. Bleck, D. Raabe (Eds.), Proc. of 2nd Int. Conf. on High Manganese Steel 2014, Aachen, 355 (2014).

[28] A. Kokosza, J. Pacyna, Arch. Metall. Mater. **55**, 4, 1001 (2010).

[29] L. Kucerova, H. Jirkova, B. Masek, Arch. Metall. Mater. **59**, 3, 1189 (2014).

[30] S. Wiewiórowska, Arch. Metall. Mater. **58**, 2, 573 (2013).